NONLINEAR CURVATURE BASIS FUNCTIONS FOR STRAIN-BASED GEOMETRICALLY NONLINEAR BEAMS FOR VERY FLEXIBLE AIRCRAFT MODELING

Francisco P. Reis[1]**, Leandro R. Lustosa**[1]**, Charles Poussot-Vassal**[2]

[1]ISAE-SUPAERO, Université de Toulouse, France
francisco.pedrosa-reis@isae-supaero.fr
leandro.lustosa@isae-supaero.fr

[2]ONERA, Université de Toulouse, France
charles.poussot-vassal@onera.fr

Keywords: Geometric nonlinearities, high-aspect-ratio wings, space curves

Abstract: This paper proposes a new parametrization of very flexible aircraft structural elements to support geometric control studies. First, a sum of basis functions is used to calculate the torsion and curvature distributions of a beam-like structural element. Secondly, the modal functions are used to determine the attitude on $SO(3)$ and the position of each point on the element, assuming constant curvatures. Finally, a simulator implementation of the method is described, along with numerical simplifying strategies.

1 INTRODUCTION

High-accuracy modeling and simulation of very flexible aircraft require extensive computing power. To avoid unnecessary complexities during control design on aeroelastic platforms, simplifications are done to reduce calculations. As described in Ref. [1], models can be divided into three levels of fidelity: low, medium, or high. Naturally, distinct design tasks (e.g., control design, fatigue investigation, flight performance analysis) require different fidelity levels in different modules. Pursuing a one-stop mathematical model for all design tasks across multiple disciplines might yield computationally inefficient outcomes. This paper seeks a reasonable abstraction level for nonlinear geometric control design purposes.

In the scientific literature, modeling and simulation tools range in varying fidelity and computational cost levels. Notable examples are SHARPy [2], UM/NAST [3], and ASWING [4], whose main goals are aeroelastic systems simulation and analysis. SHARPy and UM/NAST can simulate structural dynamics and aerodynamics while offering models of different fidelity levels through the interconnection of free-flying nonlinear beam-like elements. Additionally, they can generate linearized systems around equilibrium points proper for high-dimensional linear control design and frequency domain analysis. Finally, they offer plug-in interfaces in varying levels of versatility for feedback controller simulation and analysis.

The aforementioned multidisciplinary simulators are composed of modules that each execute specific functionalities. To achieve a simulator with such a level of complexity, the different modules need to be developed and fit into a larger simulator architecture. A common shape parametrization definition avoids potentially frequent and costly shape description translations in-between modules. This article proposes a new curvature-based shape parametrization model

fit for nonlinear geometric control. A similar curvature-based approach to structural modeling is the Modal Rotations Method (MRM) [5], but the latter uses Finite Elements and the curvatures of linear displacement modes. This approach has been used in different studies, e.g., the aforementioned simulators [2–4], and most other work based on Ref. [6], due to the possibility of describing shapes beyond the linear domain.

The similarity between the tools and methods mentioned previously is that they all break down the aircraft's structural components and use either Finite Elements or discrete models to simplify the analysis of individual beam-like structural element mechanics and their interactions. By doing so, a large number of states are created. Subsequent studies are still possible on higher-order systems at the expense of a substantial increase in required computing power. Alternatively, model reduction techniques can generate lower-order models that are easier to manipulate.

In our control design context, the main setback of model reduction methods is the difficulty of comparing the resulting models created in different initial conditions. This calls for a new reduction step whenever the system is too far from its previous operating point. While control design for multiple models in multiple trim points is appropriate for gain-scheduling control techniques, this work focuses on supporting nonlinear geometric methods, thus avoiding model switching.

One alternative to reduce the number of system states is to find an appropriate nonlinear parametrization. To achieve this, constraints between variables need to be identified and introduced. Identified constraints are physical constraints and yield increased model fidelity given their implicit existence. Introduced constraints are assumptions made about the system and affect the model's accuracy. Movement constraints and allowed spacial configurations are encoded herein through superposition of carefully chosen basis functions.

The notion of wing shape superposition in $SO(3)$, i.e., the group of rotations, is ill-defined since $SO(3)$ does not configure a vector space (e.g., rotations are not commutative). Reference [7] artificially achieves superposition by adding up Euler angle basis functions. However, generating almost-global asymptotic stable controllers for Euler angles representation is complicated. Therefore, we study curvatures and torsion constraints, which are naturally commutative, and configure a coordinate-free vector space appropriate for geometric control.

This paper is organized as follows. The mathematical modeling considering the discussed constraints is presented in Sec. 2, and a simulator architecture suggestion is described in Sec. 3. To conclude, Sec. 4 presents final remarks and ways forward.

2 MODELING

2.1 Structural elements

Based on Ref. [8], we model the aircraft wing deformation as a 1-dimensional specialized beam element but with only three local strain degrees of freedom: torsion (or twist), in-plane bending, and out-of-plane bending (we drop the span-wise extension degree of freedom for simplicity). The element's neutral axis uses a reference curve to track the structural element shape. A coordinate s determines the position along the reference curve, sweeping from 0 to the beam element length. The plane perpendicular to the curve in the neutral position is assumed to stay perpendicular to the curve independently of the element's deformation.

When discussing the beam element deformation, two related notions will be important: the descriptions of torsion and curvature from differential geometry space curves and the definitions of twist and bending from continuum mechanics. Torsion and curvature are two scalar fields necessary to determine a space curve shape. According to the fundamental theorem of space curves, this concept is similar to the idea of strain in Ref. [9]. This space curve describes the deformed shape of the reference curve (also denominated herein the neutral axis). And the deformation of the reference curve infers both twist and bending, which determine the distribution of strain and stress present along the beam element.

2.2 Reference frames

From the reference curve, a reference frame is defined as follows: the x-axis aligns with the reference curve on the wing (torsion direction), the y-axis points to the leading edge (out-of-plane bending direction), and the z-axis points to the result of their cross-product (in-plane bending direction).
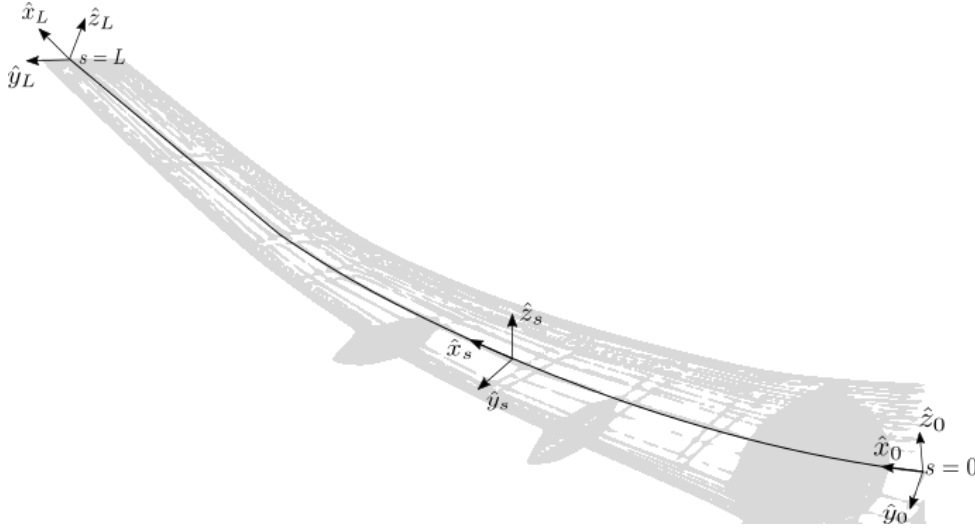

Figure 1: Reference frames of three different points on the reference curve at a deformed shape.

2.3 Deformation Modeling

Attitudes along the reference curve will be represented by a deformation map $D(s,t) : \mathbb{R}^2 \to SO(3)$, where $s \in \mathbb{R}$, $t \in \mathbb{R}$, and $D \in SO(3)$ are, respectively, the wing station (continuous) arc length coordinate (see Fig. 1), time instant, and local rotation deformation. The first partial derivative of interest is

$$\frac{\partial}{\partial t}D(s,t) = -[\boldsymbol{\Omega}(s,t)\times]D(s,t) \tag{1}$$

where $\boldsymbol{\Omega} \in \mathbb{R}^3$ is the wing station angular velocity, and $[\boldsymbol{\Omega}\times]$ is its associated left vector product operator. This value is what a rate-gyro sensor attached to that station would read. The second partial derivative of interest is

$$\frac{\partial}{\partial s}D(s,t) = -[\boldsymbol{K}(s,t)\times]D(s,t) \tag{2}$$

where $\boldsymbol{K} \in \mathbb{R}^3$ is the wing station total curvature (the grouping of torsion τ and curvature κ), and $[\boldsymbol{\Omega}\times]$ is its associated left vector product operator. At this point, we define a total twist decomposition as

$$\boldsymbol{K}(s,t) = \sum_{i=1}^{N} K_i(t)\tilde{\boldsymbol{K}}_i(s) \tag{3}$$

3

where $\tilde{\boldsymbol{K}}_i(s) \in \mathbb{R}^3$ and $K_i(t) \in \mathbb{R}$ are, respectively, N total curvature basis functions and associated total curvature weights.

2.4 Static Shape Determination

For a given set of total curvature basis functions and weights, the reference curve shape needs to be determined. The variation of deformation map D is described by Eq. (2). Once D is determined, the space curve is established by integrating the x-axis vector times ds along the reference curve. Since the x-axis is present on the top row of the D matrix, it will be equivalent to the first column of D^T. Hence, we get

$$p(s,t) = \int_0^s D^T(S,t) \begin{bmatrix} 1 \\ 0 \\ 0 \end{bmatrix} \mathrm{d}S \tag{4}$$

where $p \in \mathbb{R}^3$ maps the position of the reference curve in relation to its origin ($s = 0$). An interesting feature is that Eq. (2) does not always have an analytical solution. Therefore, for its computation, we propose the following approximation.

2.5 Constant Total Curvature Elements Approximation

An approximation is made by dividing the beam element into smaller discrete pieces. This paper assumes constant curvature along the pieces (e.g., the average between the total curvatures at the edge of the piece). Accordingly, we use the following known result [9]

$$D(s) = e^{-[\boldsymbol{K}\times]s} D_0 \tag{5}$$

where $\boldsymbol{K}$ is the constant total curvature value and D_0 is the $SO(3)$ attitude matrix at $s = 0$ along the reference curve. Terms dependent on time t have been ignored since this analysis focuses on static shape determination. Since matrix $[\boldsymbol{K}\times]$ is skew-symmetric by definition, the whole exponential term will be skew-symmetric. For the exponential of skew-symmetric matrices, the Rodrigues' Rotation Formula yields

$$e^{-[\boldsymbol{K}\times]s} = I_3 - \frac{\sin(\alpha s)}{\alpha}[\boldsymbol{K}\times] + \frac{1 - \cos(\alpha s)}{\alpha^2}[\boldsymbol{K}\times]^2 \tag{6}$$

where α is the total curvature Euclidean norm. For notation simplicity, torsion τ is represented as K_x and curvature κ is represented in its y and z projections. Therefore,

$$\alpha = \sqrt{K_\mathrm{x}^2 + K_\mathrm{y}^2 + K_\mathrm{z}^2} \tag{7}$$

Once the calculation for the deformation map D is done, then the reference curve shape is calculated using Eq. (4) to obtain

$$p(s) = \int_0^s D_0^T \left(e^{-[\boldsymbol{K}\times]S}\right)^T \begin{bmatrix} 1 \\ 0 \\ 0 \end{bmatrix} \mathrm{d}S \tag{8}$$

where the time t is omitted due to the static calculation hypothesis. After rearrangement, we obtain

$$p(s) = D_0^T \int_0^s \left(e^{-[\boldsymbol{K}\times]S}\right)^T \mathrm{d}S \begin{bmatrix} 1 \\ 0 \\ 0 \end{bmatrix} \tag{9}$$

Using the Rodrigues' rotation formula, applying the transpose and using the α definition from Eq. (7), we obtain

$$p(s) = D_0^T \left(I_3 \int_0^s \mathrm{d}S + \frac{[\boldsymbol{K}\times]}{\alpha} \int_0^s \sin{(\alpha S)}\mathrm{d}S + \frac{[\boldsymbol{K}\times]^2}{\alpha^2} \int_0^s (1 - \cos{(\alpha S)})\,\mathrm{d}S \right) \begin{bmatrix} 1 \\ 0 \\ 0 \end{bmatrix} \quad (10)$$

Solving the integrals above yields

$$p(s) = D_0^T \left(sI_3 + \frac{[\boldsymbol{K}\times]}{\alpha} \frac{(-\cos{(\alpha s)} + 1)}{\alpha} + \frac{[\boldsymbol{K}\times]^2}{\alpha^2} \left(s - \frac{\sin{(\alpha s)}}{\alpha} \right) \right) \begin{bmatrix} 1 \\ 0 \\ 0 \end{bmatrix} \quad (11)$$

Finally, taking advantage of the special relation for left vector product operators, i.e.,

$$[\boldsymbol{K}\times]^2 = \boldsymbol{K}\boldsymbol{K}^T - \alpha^2 I_3 \quad (12)$$

and by rearranging terms, we have

$$p(s) = D_0^T \left(\frac{s\boldsymbol{K}\boldsymbol{K}^T}{\alpha^2} - \frac{[\boldsymbol{K}\times](\cos{(\alpha s)} - 1)}{\alpha^2} - \frac{\sin{(\alpha s)}[\boldsymbol{K}\times]^2}{\alpha^3} \right) \begin{bmatrix} 1 \\ 0 \\ 0 \end{bmatrix} \quad (13)$$

The method proposed above is a numerical method derived from the Euler method. Alternatively, for a pure first-order Euler method a function f would be defined as

$$\frac{\partial}{\partial s}D(s) = -[\boldsymbol{K}(s)\times]D(s) = f(s, D(s)) \quad (14)$$

The first-order Euler method considers $f(s, D(s))$ constant on the whole discrete segment. In our proposal, instead, the total curvature $\boldsymbol{K}$ was considered constant. This assumption reshaped the equation to allow for an exponential solution that can be calculated by the relatively simple Rodrigues' rotation formula.

Another benefit of the proposed method is that $D(s)$ won't numerically diverge from $SO(3)$. This happens because the exponential of a skew-symmetric matrix is part of $SO(3)$, and D_0 is already part of $SO(3)$. By consequence, the result of their multiplication $D(s)$ is also in $SO(3)$. This is already expected for $D(s)$; nevertheless, other numerical solutions may diverge faster from orthogonal matrices, requiring more frequent corrective procedures. Because of the aforementioned advantages, this numerical method has been chosen for this study.

3 SIMULATOR

During this study, a static simulator was coded to simulate the wing's deformed shape. This simulator is intended to be the first part of a larger aeroelastic simulator, similar to the ones mentioned in the introduction but with the specific objective of facilitating control analysis and design. Currently, the simulator is only capable of calculating the static shape based on the equations shown in Sec. 2.5.

Albeit only able to run static conditions, for the time being, the code separates two types of inputs: time-varying (represented as ellipses in Fig. 2) and constant (represented as rounded rectangles in Fig. 2). Time-varying inputs include the total curvature basis weights ($K_i(t)$ from Eq. (3)), which will represent the shape states of the final dynamic simulator. Constant inputs includes properties inherent to the wing, such as the total curvature basis functions ($\tilde{\boldsymbol{K}}_i(s)$ from Eq. (3)) or the attachment point (or where $s = 0$) for the structural element under analysis.

As outputs, the simulator provides both the reference curve position in relation to its origin ($p(s)$ from Eq. (13)) and the deformation map ($D(s)$ from Eq. (5)).

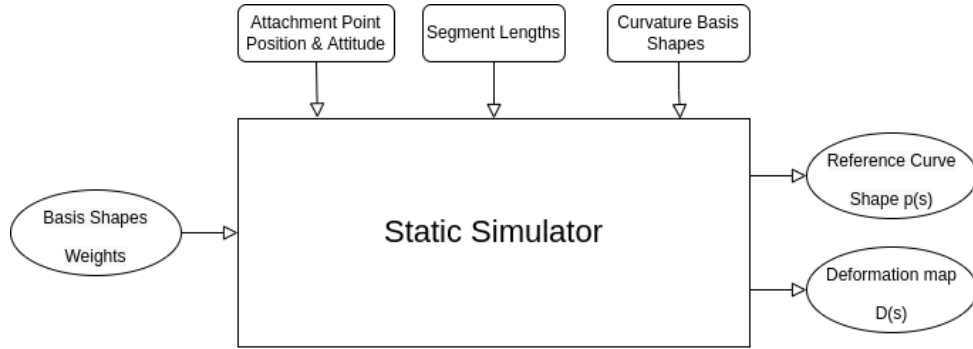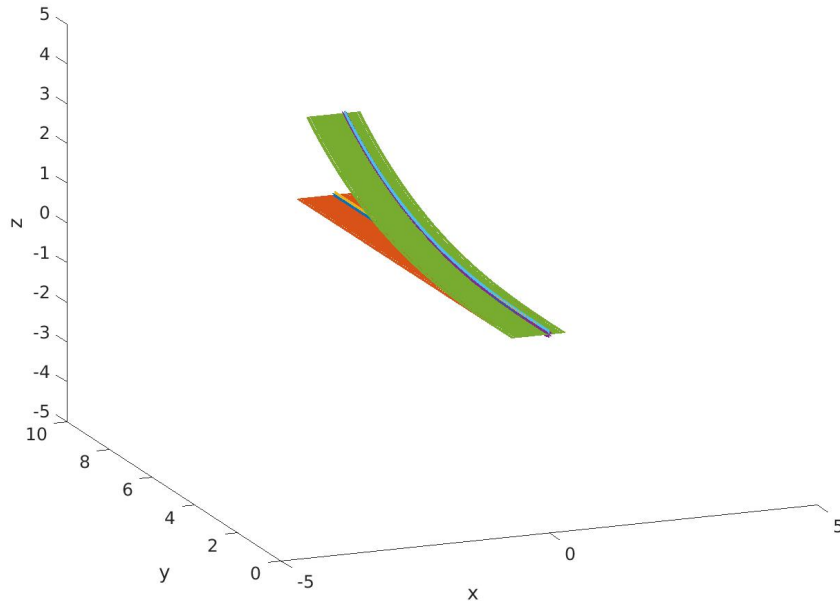Figure 2: Current simulator diagram.

Figure 3: Simulator example output with an exaggerated first bending mode.

3.1 Small-angle approximations

Another possible simplification when using the Rodrigues' Rotation Formula, shown for our specific case in Eq. (6), is to apply two different small-angle approximations. The first one is the sine function approximation $\sin{(\theta)} \approx \theta$ on the second term of the equation

$$e^{-[\boldsymbol{K}\times]s} = I_3 - s[\boldsymbol{K}\times] + \frac{1 - \cos{(\alpha s)}}{\alpha^2}[\boldsymbol{K}\times]^2 \tag{15}$$

6

The second approximation that can be used is $\cos\left(\theta\right) \approx 1 - \frac{\theta^2}{2}$, resulting in

$$e^{-[\boldsymbol{K}\times]s} = I_3 - s[\boldsymbol{K}\times] + \frac{\left(s[\boldsymbol{K}\times]\right)^2}{2} \tag{16}$$

Similarly, the curve shape calculation (Eq. (13)) can also be simplified to read

$$p(s) = D_0^T \left(\frac{s\boldsymbol{K}\boldsymbol{K}^T}{\alpha^2} + \frac{[\boldsymbol{K}\times]s^2}{2} - \frac{s[\boldsymbol{K}\times]^2}{\alpha^2} \right) \begin{bmatrix} 1 \\ 0 \\ 0 \end{bmatrix} \tag{17}$$

One more employment of the left vector product property shown in Eq. (12) yields

$$p(s) = D_0^T \left(sI_3 + \frac{[\boldsymbol{K}\times]s^2}{2} \right) \begin{bmatrix} 1 \\ 0 \\ 0 \end{bmatrix} \tag{18}$$

The angle under consideration in the approximation is the multiplication of α (the total curvature Euclidean norm) by s (the beam element length). As a result, the length of the segments of constant total curvature can be dynamically chosen to always keep the total segment angle inside an acceptable range for the approximation. The user's expected precision should define this range.

3.2 Parallel computation

One advantage of the proposed formulation is that the calculation of each section is independent of its neighbours. This enables each section calculation to be done in parallel, decreasing the necessary computing time. By lowering the computational load, the hardware requisites will also be lesser, facilitating the implementation of this algorithm into an embedded system if needed in optimization solvers for control purposes.

4 CONCLUSIONS

This article aims to present a preliminary study on a new parametrization specifically developed to facilitate geometric control design and analysis. The necessary modeling has been described, explaining the structural element properties, the reference frames used in the modeling, the equations behind the deformation map, and the deformed static shape. Since the equation does not have analytical solutions, an approximation using smaller elements with constant total curvature has been shown to allow the implementation of the method in question. Then, more details on an implementation example has been presented, discussing numerical and implementation strategies that can be used to facilitate the creation of a demonstrator.

Further work needs to be done to enrich the formulation described. An estimation algorithm must be developed to allow for the total curvature weights estimation, allowing for a live shape estimation for active control purposes. Then, structural and aerodynamics equations need to be added to allow the execution of dynamic simulations. Adaptions and checks will be done to the shape estimator to account for changes related to a dynamic application.

5 REFERENCES

[1] Afonso, F., Vale, J., Oliveira, E., et al. (2017). A review on non-linear aeroelasticity of high aspect-ratio wings. *Progress in Aerospace Sciences*, 89, 40–57. ISSN 03760421. doi:10.1016/j.paerosci.2016.12.004.

[2] Carre, A. d., Muñoz-Simón, A., Goizueta, N., et al. (2019). SHARPy: A dynamic aeroelastic simulation toolbox for very flexible aircraft and wind turbines. *Journal of Open Source Software*, 4(44), 1885. ISSN 2475-9066. doi:10.21105/JOSS.01885.

[3] Su, W. and Cesnik, C. E. S. (2010). Nonlinear aeroelasticity of a very flexible blended-wing-body aircraft. *Journal of Aircraft*, 47(5). doi:10.2514/1.47317.

[4] Drela, M. (1999). Integrated simulation model for preliminary aerodynamic, structural, and control-law design of aircraft. *40th Structures, Structural Dynamics, and Materials Conference and Exhibit*.

[5] Drachinsky, A. and Raveh, D. E. (2020). Modal rotations: A modal-based method for large structural deformations of slender bodies. *AIAA Journal*, 58(7), 3159–3173. ISSN 00011452. doi:10.2514/1.J058899.

[6] Hodges, D. H. (2012). Geometrically exact, intrinsic theory for dynamics of curved and twisted anisotropic beams. *https://doi.org/10.2514/2.2054*, 41(6), 1131–1137. ISSN 00011452. doi:10.2514/2.2054.

[7] Lustosa, L. R., Kolmanovsky, I., Cesnik, C. E., et al. (2021). Aided inertial estimation of wing shape. *Journal of Guidance, Control, and Dynamics*, 44(2), 210–219. ISSN 15333884. doi:10.2514/1.G005368.

[8] Cesnik, C. E. and Brown, E. L. (2003). Active warping control of a joined-wing airplane configuration. *Collection of Technical Papers - AIAA/ASME/ASCE/AHS/ASC Structures, Structural Dynamics and Materials Conference*, 4, 2847–2861. ISSN 02734508. doi:10.2514/6.2003-1715.

[9] Cesnik, C. E. S. and Su, W. (2005). Nonlinear aeroelastic modeling and analysis of fully flexible aircraft. In *46th AIAA/ASME/ASCE/AHS/ASC Structures, Structural Dynamics and Materials Conference*. Reston, Virigina: American Institute of Aeronautics and Astronautics. ISBN 978-1-62410-065-9. doi:10.2514/6.2005-2169.

COPYRIGHT STATEMENT